Low frequency resistance and critical current fluctuations in Al-based Josephson junctions

C. D. Nugroho,[1, a)] V. Orlyanchik,[1] and D. J. Van Harlingen[1]
Department of Physics and Materials Research Laboratory, University of Illinois at Urbana-Champaign, Urbana, Illinois 61801, USA

We present low-temperature measurements of the low-frequency $1/f$ noise arising from an ensemble of two-level fluctuators in the oxide barrier of Al/AlO$_x$/Al Josephson junctions. Both the critical-current noise (S_{I_c}/I_c^2) and normal-state resistance noise (S_{R_n}/R_n^2) scale linearly in temperature with the same noise magnitude, implying an equivalence between the two. Combining our noise results with those from other laboratories and junction architectures, we deduce the scaling $\frac{S_{R_n}}{R_n^2} \equiv \frac{S_{I_c}}{I_c^2} \approx \frac{1}{A/\mu m^2}\left(\frac{T}{1\text{ K}}\right) \times 10^{-13}$ Hz^{-1}. We find that the density of two-level fluctuators in the junction barrier is similar to the typical value in glassy systems. We discuss the implications and consistency with recent qubit experiments.

Recent progress in superconducting qubits have resulted in longer coherence times. How far this improvement can continue depends crucially on the losses intrinsic to the Josephson junction. Qubit energy spectroscopy have revealed a density of avoided level crossings arising from the interaction of the qubit with two-level systems (TLSs) in the junction barrier[1–3]. Additionally, critical-current fluctuations in Josephson junctions are known to exhibit a low-frequency $1/f^\alpha$ ($\alpha \sim 1$) spectrum[4,5], which is generally understood to arise from a collection of TLSs in the tunnel barrier[6,7]. The precise microscopic origin of these TLSs and the coupling mechanisms remain relatively unknown.

A survey of a variety of junction architectures from several laboratories found the low frequency $1/f$ critical-current noise spectral density, S_{I_c}, to have an almost universal magnitude at $T = 4.2$ K [8]. By postulating a T^2 temperature dependence based on noise measurements in dc SQUIDs[9] an almost universal noise characteristic was proposed: $S_{I_c}/I_c^2(f = 1Hz) \approx 1.44 \times 10^{-10}(T/4.2\text{ K})^2$ Hz^{-1}.

However, results on the tunneling resistance noise[10], S_{R_n}/R_n^2, in Al/AlO$_x$/Al shadow junctions showed a linear temperature dependence. The noise magnitude can be compared through the Ambegaokar-Baratoff relation, $I_cR_n = \pi\Delta/2e \tanh\left(\frac{\Delta}{2k_BT}\right)$, which implies an equivalent critical-current noise at 4.2 K that is three orders of magnitude lower than previous S_{I_c} measurements. This apparent discrepancy between S_{I_c} and S_{R_n} led to the proposal of a Kondo-traps noise mechanism[11,12] that could account for the excess noise magnitude and T^2 dependence in the SC state.

Furthermore, recent measurements of the kinetic inductance noise[13] S_L/L^2 of Al shadow junctions at $T = 25$ mK placed an even lower bound to the noise magnitude than previous measurements of S_{I_c} and S_{R_n}.

To clarify the apparent discrepancy, in this Letter we present extensive measurements of both S_{I_c} and S_{R_n} in Al/AlO$_x$/Al junctions, the material system most relevant in current superconducting qubits. Our measurements show an equivalence between S_{I_c}/I_c^2 and S_{R_n}/R_n^2 as expected from the Ambegaokar-Baratoff relation. We find a linear temperature dependence in all devices and a noise magnitude that is consistent with previous measurements in Al-shadow junctions[10]. Our results place an upper limit on the proposed additional Kondo-traps noise contribution. Combining our results with those from other laboratories[10,14] and junction architectures we suggest a scaling relation for noise in AlO$_x$ based junctions. We discuss the implications for superconducting qubits and the consistency with recent qubit measurements.

We fabricated shunted and unshunted Al/AlO$_x$/Al Josephson junctions using either the double-angle shadow evaporation or the cross technique. In double-angle evaporation the junction electrodes and barrier oxidation are completed in one step without breaking vacuum. In the cross technique the electrodes are deposited in two evaporation steps. In the second evaporation step the base electrode is ion-milled to remove surface contaminants, followed by the controlled oxidation of the junction barrier and the top electrode evaporation. Both junction architectures were completed in a chamber with a base pressure of $\approx 3 \times 10^{-10}$ Torr. For the shunted junctions the shunt resistors were fabricated by e-beam evaporating 60 nm of Pd, with typical low temperature sheet resistances $R_s \approx 1.3\ \Omega$/sq. The shunt resistors are patterned with large, $300 \times 300\ \mu$m^2, cooling fins to minimize hot-electron effects[15].

Measurements of the critical current noise S_{I_c} were performed in a bridge configuration (Fig. 1A inset) with a dc SQUID monitoring the current fluctuations across the two bridge arms. A small $R_{std} \approx 0.5\ \Omega$ is placed in series with the SQUID pickup loop. The two junctions in the bridge are matched and fabricated on-chip in the same lithography step. Potentiometers at room-temperature are used to adjust the currents through the junctions, while the dc-SQUID monitored the voltage imbalance, which is typically kept at zero.

Since the critical-current noise in the junctions are uncorrelated, their noise power contributions add to give

[a)] Electronic mail: nugroho2@illinois.edu

the total noise seen at the SQUID:

$$S_I^{sq} = \frac{R_{D1}^2}{(R_{std}+R_{D1}+R_{D2})^2}\left(\frac{I_{c1}}{I_1}\right)^2 S_{I_{c1}} + \frac{R_{D2}^2}{(R_{std}+R_{D1}+R_{D2})^2}\left(\frac{I_{c2}}{I_2}\right)^2 S_{I_{c2}}, \quad (1)$$

where I_i, I_{ci}, and $R_{Di} = \partial V_i/\partial I_i$ are respectively the bias current, critical current and the dynamic resistance of the ith junction. When the junctions are closely matched, $R_{D1} \approx R_{D2} = R_D$, and are biased near I_c, $I_c/I_b \approx 1$, the noise seen by the SQUID is given by:

$$S_I^{sq} = \frac{1}{2} S_{I_c}, \quad (2)$$

where $S_{I_c} = \frac{1}{2}(S_{I_{c1}} + S_{I_{c2}})$, is the averaged critical-current noise power density across the two junctions. The reduction by a factor of two in the noise power sensitivity compared to the standard SQUID potentiometry technique[9] is more than compensated by the attenuation of common-mode noise sources such as spurious temperature fluctuations and external biasing noise.

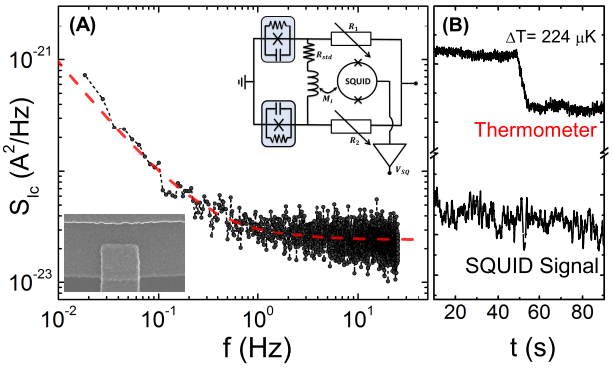

FIG. 1. (A) Critical current power spectrum measured at $T = 315$ mK, and $I_b/I_c = 1.05$. The dashed line is a fit to $1/f+$ a white noise component. Top inset: Schematic representation of the bridge-SQUID potentiometry circuit. Bottom inset: SEM image of the Al/AlO$_x$/Al junctions. (B) Time traces of the sample temperature and the SQUID signal, monitored across a small temperature perturbation at $T = 315$ mK for $I_b/I_c = 1.05$.

In double-angle evaporated junctions the critical currents can be matched to within 1%, allowing for a high attenuation of small temperature fluctuations ~ 100s μK (Fig. 1B). The residual signal from common temperature fluctuations can be detected when the fluctuations exceed ~ 1 mK, which is much larger than the typical thermal instabilities of the system (examined in detail in Ref. 16.

The system background noise, S_{BG}, was determined by monitoring the SQUID output while keeping the junctions in the superconducting state (zero bias). In this regime the high-frequency, $f > 10$ Hz, noise spectrum is dominated by the Johnson noise of the standard resistor, while the low-frequency, $f < 10$ Hz spectrum is dominated by the $1/f$ flux noise of the SQUID and feedback electronics. A base $1/f$ equivalent flux noise of $S_\Phi^{1/2}(1Hz) \approx 6\mu\Phi_o/\sqrt{\text{Hz}}$ is observed, consistent with the calibration data for the SQUID sensor. The S_{BG} is subtracted from the measured data and the remainder is attributed to fluctuations in the junctions.

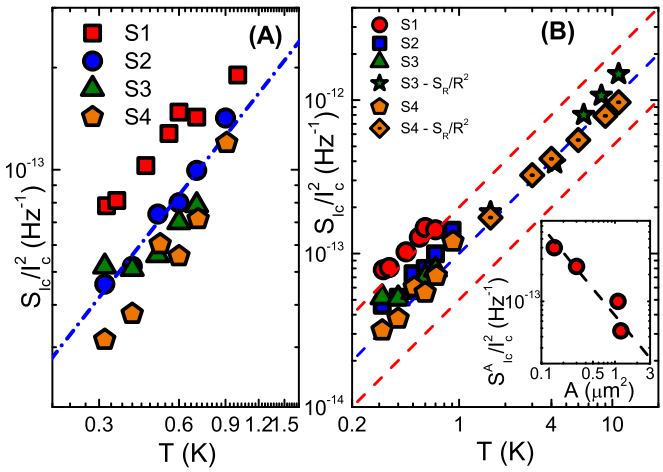

FIG. 2. Temperature dependence S_{I_c}/I_c^2 (A) and S_{I_c}/I_c^2 with S_{R_n}/R_n^2 (B) at $f = 1$ Hz in several sets of devices. The noise values are area normalized to $A = 1$ μm^2. The dashed line shows linear T dependence (see text). Inset: Critical current noise (not area normalized), $S_{I_c}^A/I_c^2$, at $T = 500$ mK as a function of junction area. The dashed line depicts $1/A$ dependence.

Fig. 1A shows noise power spectral density for device S1 taken at $T = 315$ mK and $I_b = 10$ μA, corresponding to $I_b/I_c \approx 1.05$. The low-frequency spectrum shows a $1/f^\alpha$ noise which crosses over to the frequency independent noise resulting from the thermal noise of the shunt and the mixed down junction quantum noise[17]. It is important to mention that for all the junctions reported here the measured values of α ranged between 0.9 to 1.1 and were independent of T. The dependence of the noise power on the junction area is shown in Fig. 2B. The inverse area scaling $(1/A)$ of the power density is consistent with noise resulting from an ensemble of uncorrelated fluctuators, with sufficient density to produce featureless $1/f$ spectrum in all measured junctions down to ≈ 0.1 μm^2. Furthermore, the $1/A$ dependence rules out spurious fluctuations induced by the bath temperature, which would have generated a noise that is independent of the junction area[16].

The normalized noise magnitude increases linearly with temperature (Fig. 2A) with average T dependence given by $S_{I_c}/I_c^2 \approx 1.3 \times 10^{-13}$ $(T/1\text{K})$ Hz^{-1} (Fig. 2A,

dashed lines). Both, the noise magnitude and the linear-T dependence are consistent with results in Nb/AlO_x/Nb trilayer junctions[14], but differed from the T^2 dependence observed in dc-SQUIDs[9].

Following the theoretical proposals in Ref. 11 and 12, the noise characteristics in the superconducting state and normal state are expected to be different. To observe directly this possible crossover we extended the noise measurement for samples S3 and S4 above the $T_c \sim 1.25$ K of Al. For $T > T_c$ the shunted junction is represented by the equivalent parallel resistance $R_{eq} = R_n R_s/(R_n+R_s)$, of R_s the shunt resistance, and R_n the tunneling resistance the unshunted junction. Assuming that the noise is dominated by fluctuations in R_n (fluctuations in R_s are small), we can relate the tunneling resistance noise S_{R_n}/R_n^2 to the signal measured by the SQUID S_I^{sq} as:

$$\frac{S_{R_n}}{R_n^2} = \frac{1}{2}\left(\frac{R_\Sigma}{R_n}\right)^2 \frac{1}{(dR_{eq}/dR_n)^2}\frac{S_I^{sq}}{I^2}, \qquad (3)$$

where R_Σ is the total resistance in the loop, which can be determined from the Johnson-Nyquist noise measured at zero bias, and I is the current bias through each of the junctions. Since $R_s < R_n$, most of the current flows through the shunt resistor, thus to measure fluctuations due to the tunneling resistance we used bias currents $I \approx 50 - 250$ μA to obtain sufficient signal visibility. To remove the ambiguity from self-heating we verified the quadratic dependence of the noise power on biasing current $S_I^{sq} \propto I^2$.

Measured S_{R_n}/R_n^2 varies linearly with temperature similar to the dependence in S_{I_c}/I_c^2, and with a noise power magnitude consistent with the equivalence $S_{I_c}/I_c^2 = S_{R_n}/R_n^2$ as expected from the Ambegaokar-Baratoff relation. Fig. 2B shows the comparison between S_{R_n} and S_{I_c}.

To rule out a contribution of the low-frequency noise from the shunt resistors we have also measured S_{R_n}/R_n^2 on a collection of unshunted junctions. The measurement of the resistance fluctuations were performed in an ac-bridge configuration as described in Ref. 10. We used first stage amplifiers with an input noise ≈ 1.6 nV/$\sqrt{\text{Hz}}$ for a 1 kΩ load impedance. For some of the junctions we have also measured the noise without the bridge layout, while still computing the cross-spectral density of the two readout branches. The modulation frequency is dictated by the sample and setup resistance and capacitance and is typically in the range $1-3$ kHz. Measurements below the T_c of Al were done by suppressing the superconductivity with an applied magnetic field, $B_\perp > 100$ mT.

The area dependence of the noise in unshunted junctions (Fig. 3A) follows $S_{R_n} \propto 1/A$, suggesting the averaging over an ensemble of uncorrelated fluctuators. The area scaling and a featureless $1/f$ spectrum are found to hold down to $A \approx 0.04$ μm^2 at $T = 2$ K, indicating a high degree of barrier uniformity. For junction areas in the limit $A \leq 0.04$ μm^2 at $T = 2$ K the noise becomes more non-gaussian leading to a deviation from the linear area scaling. At even smaller junction areas the noise is dominated by distinct two level systems, where the noise magnitude at 1 Hz is generally lower than that expected from the $\propto 1/A$ scaling. The detailed dynamics of the fluctuator and transition to $1/f$ noise is beyond the scope of this letter and will be discussed elsewhere.

Fig. 3B shows the dependence of area normalized S_{R_n} on temperature. The three dashed lines in Fig. 3B represent the upper and lower bounds, and the average S_{R_n}/R_n^2 magnitude of the noise. The average noise magnitude over all the junctions is well fitted by $S_{R_n}^{\text{av}}/R_n^2 = 1 \times 10^{-13}$ $(T/1\text{K})$ Hz^{-1}, while the upper and lower bounds differ by a factor of two from this value. Part of the spread can be explained by the uncertainty in the junction sizes. The averaged tunneling-resistance noise and the observed upper and lower limits are consistent with the measured critical-current noise as shown by the dashed lines in Fig. 2B. For $T \approx 70$ K we observed a deviation from the linear temperature scaling, which may indicate the thermal activation of additional noise mechanisms.

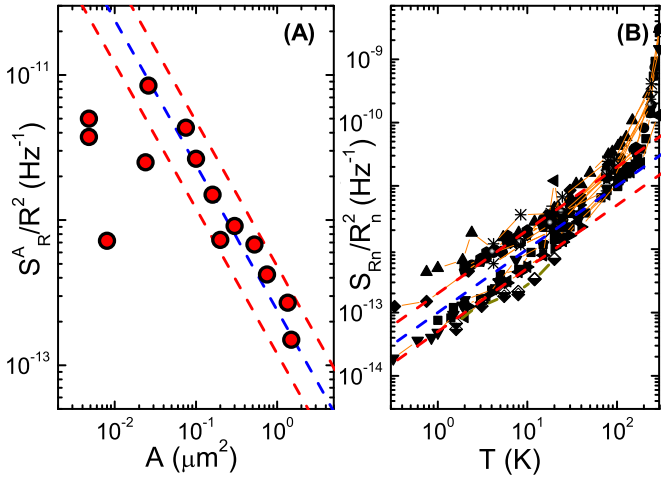

FIG. 3. (A) Area dependence of the $S_{R_n}/R_n^2(f = 1$ Hz) in unshunted junctions at $T = 2$ K. Note the deviation from the linear scaling at $A \sim 0.04\mu$m^2. (B) Temperature dependence of S_{R_n}/R_n^2 in unshunted junctions. The noise value is quoted at $f = 1$ Hz and is area normalized to $A = 1$ μm^2. The dashed lines depict the average noise value as well as its upper and lower bounds (see text).

Among the important questions is the location of the fluctuating TLSs. We note that recent noise measurements in junctions with AlO_x barriers and Nb electrodes[14] showed similar noise magnitude and a linear temperature dependence. Additionally, we measured identical noise characteristics in double-angle evaporated AlO_x junctions with $\sim$ 1 nm of Ag deposited on the AlO_x-Al interface. Lastly, the same noise behavior is observed even in the AlO_x cross junction where the barrier is oxidized after an aggressive ion milling of the surface. These properties suggest that the noise sources are insensitive to the barrier interfaces and that the main contribution comes from TLSs buried within the amor-

phous AlO_x barrier. Most likely the TLSs correspond to atoms that tunnel between two positions in the barrier modifying locally tunneling probability. Combining our results with measurements from different laboratories and various junction architectures lead to the empirical formula for T dependence of the $1/f$ noise in AlO_x based junctions:

$$\frac{S_{R_n}}{R_n^2} = \frac{S_{I_c}}{I_c^2} \approx \frac{1}{A/\mu m^2}\left(\frac{T}{1\text{ K}}\right) \times \frac{1}{f} \times 10^{-13}\text{ Hz}^{-1} \quad (4)$$

The low-frequency noise properties measured here can be used to estimate the density of TLSs in the amorphous AlO_x. Gaussian featureless $1/f$ spectrum requires the averaging of $\sim 1-2$ active fluctuators per frequency octave[18]. In our measurements we observed a crossover from featureless $1/f$ and the onset of non-gaussianity for junctions with $A \leq 0.04\ \mu m^2$ at $T = 2$ K. Assuming that the $1/f$ noise persists in the frequency range $1\ \mu$Hz $- 1$ THz (~ 60 octaves), the estimated density of fluctuators at $T = 1$ K is $\rho_{TLS} \sim 10^{17} - 10^{18}$ cm^{-3} K^{-1}. This estimate is similar to the almost universal density of TLSs in glassy systems[19,20], and consistent with the density of TLSs inferred from the number of avoided level crossings in qubit energy spectroscopy[2,21,22] - ~ 0.5 GHz^{-1} μm^{-2}.

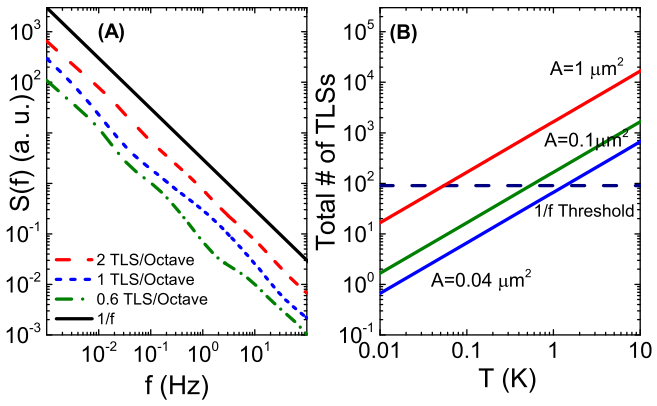

FIG. 4. (A) Simulated noise resulting from averaging over different number of TLSs per frequency octave. (B) Amount of fluctuators extracted from measured $1/f$ noise as function of temperature for several junction sizes. Dashed line shows statistical threshold for featureless $1/f$ noise.

Fig. 4B plots the total number of active TLSs in the barrier as a function of temperature assuming the estimated TLS density. The threshold which may be relevant for qubit architectures is set by having only a few TLSs in the entire tunnel barrier. For temperatures $T \approx 50$ mK and a junction size $A \sim 0.01\ \mu m^2$, which is the size of the junctions in transmon[23] and flux qubits[1], the average number of TLSs is estimated to be less than one. This size threshold is consistent with the high intrinsic quality factor of the junctions observed in 3D transmon[24] and measurements of the junction kinetic inductance noise[13]. Additionally, recent measurements of the free induction decay in 3D Transmons have shown a ~ 15 kHz beating in the qubit frequency, which would be consistent with the presence of one active TLS in the junction[25].

Following the arguments of Ref. 11 we derive:

$$\frac{S_{I_c}}{I_c^2}(f) \approx (\delta A)^2 \rho t \frac{1}{A}\frac{T}{f}, \quad (5)$$

where $\delta I_c = I_c(\delta A/A)$, δA parameterizes the effective change in the area of the junction, $t \approx 1-2$ nm is the tunnel barrier thickness and ρ is the density of TLSs. Using the density of TLSs obtained previously and the measured noise magnitude, we estimate the effective change in the area of the junction to be $\delta A \sim 0.1 - 0.3$ nm^2, consistent with Ref. 10 and 11.

In summary, we have measured both the critical current and tunnel resistance noise in $Al/AlO_x/Al$ Josephson junctions, the material commonly used in qubits. The measurements uphold the equivalence $S_{I_c}/I_c^2 = S_{R_n}/R_n^2$ with a linear temperature dependence down to the lowest temperatures measured. The estimated TLS density is consistent with observations from qubit energy spectroscopy.

This research was funded by the Office of the Director of National Intelligence (ODNI), Intelligence Advanced Research Projects Activity (IARPA), through the Army Research Office. All statements of fact, opinion, or conclusions contained herein are those of the authors and should not be construed as representing the official views or policies of IARPA, the ODNI, or the U.S. Government.

[1] B. L. T. Plourde, T. L. Robertson, P. A. Reichardt, T. Hime, S. Linzen, C. E. Wu, and J. Clarke, Phys. Rev. B. **72**, 060506(R) (2005).
[2] M. J. A. Stoutimore, M. S. Khalil, C. J. Lobb, and K. D. Osborn, App. Phys. Lett. **101**, 062602 (2012).
[3] J. Lisenfeld, C. Muller, J. H. Cole, P. Bushev, A. Lukashenko, A. Shnirman, and A. V. Ustinov, Phys. Rev. Lett. **105**, 230504 (2010).
[4] B. Savo, F. C. Wellstood, and J. Clarke, Appl. Phys. Lett. **50**, 1757 (1987).
[5] V. Foglietti, W. J. Gallagher, M. B. Ketchen, A. W. Kleinsasser, R. H. Koch, S. I. Raider, and R. L. Sandstrom, Appl. Phys. Lett. **49**, 1393 (1986).
[6] P. Dutta and P. M. Horn, Rev. Mod. Phys. **53**, 497 (1981).
[7] C. T. Rogers and R. A. Buhrman, IEEE Transactions on Magnetics **MAG-19**, 453 (1983).
[8] D. J. V. Harlingen, T. L. Robertson, B. L. T. Plourde, P. A. Reichardt, T. A. Crane, and J. Clarke, Phys. Rev. B **70**, 064517 (2004).
[9] F. C. Wellstood, C. Urbina, and J. Clarke, Appl. Phys. Lett. **85**, 22 (2004).
[10] J. Eroms, L. C. van Schaarenburg, E. F. C. Driessen, J. H. Plantenberg, C. M. Huizinga, R. N. Schouten, A. H. Verbruggen, C. J. P. M. Harmans, and J. E. Mooij, Appl. Phys. Lett. **89**, 122516 (2006).
[11] L. Faoro and L. B. Ioffe, Phys. Rev. B **75**, 132505 (2007).
[12] M. H. Ansari and F. K. Wilhelm, Phys. Rev. B **84**, 235102 (2011).
[13] K. W. Murch, S. J. Weber, E. M. Levenson-Falk, R. Vijay, and I. Siddiqi, Appl. Phys. Lett. **100**, 142601 (2012).
[14] S. Pottorf, V. Patel, and J. E. Lukens, Appl. Phys. Lett. **94**, 043501 (2009).
[15] F. C. Wellstood, C. Urbina, and J. Clarke, Phys. Rev. B **49**, 5942 (1994).

[16] S. M. Anton, C. D. Nugroho, J. S. Birenbaum, S. R. O'Kelley, and V. Orylanchik, Appl. Phys. Lett. **101**, 092601 (2012).
[17] R. H. Koch, D. J. V. Harlingen, and J. Clarke, Phys. Rev. Lett. **45** (1980).
[18] P. J. Restle, *1/f noise in semiconductors and metals*, Ph.D. thesis, University of Illinois at Urbana-Champaign (1986).
[19] C. C. Yu, J. Low Temp. Phys. **137** (2004).
[20] W. A. Phillips, Rep. Prog. Phys. **50**, 1657 (1987).
[21] J. M. Martinis, K. B. Cooper, R. McDermott, and M. Steffen, Phys. Rev. Lett. **95**, 210503 (2005).
[22] J. S. Kline, H. Wang, S. Oh, J. M. Martinis, and D. P. Pappas, Supercond. Sci. Technol. **22**, 015004 (2009).
[23] J. A. Schreier, A. A. Houck, J. Koch, D. I. Schuster, B. R. Johnson, J. M. Chow, J. M. Gambetta, J. Majer, L. Frunzio, M. H. Devoret, S. M. Girvin, and R. J. Schoelkopf, Phys. Rev. B **77**, 180502(R) (2008).
[24] H. Paik, D. I. Schuster, L. S. Bishop, G. Catelani, A. P. Sears, B. R. Johnson, M. J. Reagor, L. Frunzio, L. Glazman, S. M. Girvin, M. H. Devoret, and R. J. Schoelkopf, Phys. Rev. Lett. **107**, 240501 (2011).
[25] R. J. Schoelkopf, (2013), private communication.